PHYSICAL REVIEW B **92**, 081107(R) (2015)

Quantized topological magnetoelectric effect of the zero-plateau quantum anomalous Hall state

Jing Wang,[1,2] Biao Lian,[1] Xiao-Liang Qi,[1] and Shou-Cheng Zhang[1,2]

[1]*Department of Physics, McCullough Building, Stanford University, Stanford, California 94305-4045, USA*

[2]*Stanford Institute for Materials and Energy Sciences, SLAC National Accelerator Laboratory, Menlo Park, California 94025, USA*

(Received 9 June 2015; published 10 August 2015)

The topological magnetoelectric effect in a three-dimensional topological insulator is a novel phenomenon, where an electric field induces a magnetic field in the same direction, with a universal coefficient of proportionality quantized in units of $e^2/2h$. Here, we propose that the topological magnetoelectric effect can be realized in the zero-plateau quantum anomalous Hall state of magnetic topological insulators or a ferromagnet-topological insulator heterostructure. The finite-size effect is also studied numerically, where the magnetoelectric coefficient is shown to converge to a quantized value when the thickness of the topological insulator film increases. We further propose a device setup to eliminate nontopological contributions from the side surface.

DOI: 10.1103/PhysRevB.92.081107 PACS number(s): 73.43.−f, 73.20.−r, 85.75.−d

The search for topological quantum phenomena has become an important goal in condensed matter physics. Topological phenomena in physical systems are determined by topological structures and are thus universal and robust against perturbations, and the electromagnetic response is usually exactly quantized [1]. Two well-known examples of topological quantum phenomena are the flux quantization in superconductors [2] and Hall conductance quantization in the quantum Hall effect (QHE) [3]. The remarkable observation of such topological phenomena is that the quantization is exact, which provide the precise values of fundamental physics constants, such as Planck's constant h [4].

The recent discovery of the time-reversal ($\mathcal{T}$) invariant (TRI) topological insulator (TI) brings the opportunity to study a large family of new topological phenomena [5,6]. The electromagnetic response of a three-dimensional (3D) insulator is described by the topological θ term [7–9] of the form

$$\mathcal{S}_\theta = \frac{\theta}{2\pi}\frac{e^2}{h}\int d^3x dt \mathbf{E}\cdot\mathbf{B}, \tag{1}$$

together with the ordinary Maxwell terms. Here, $\mathbf{E}$ and $\mathbf{B}$ are the conventional electromagnetic fields inside the insulator, e is the charge of an electron, and θ is the dimensionless pseudoscalar parameter describing the insulator, which refers to the axion field in particle physics [10]. Under the periodic boundary condition, all physical quantities are invariant if θ is shifted by integer multiples of 2π. Therefore, all TRI insulators are described by either $\theta = 0$ or $\theta = \pi$ (modulo 2π). TIs are defined by $\theta = \pi$, which cannot be connected continuously to trivial insulators, defined by $\theta = 0$, by TRI perturbations. With an open boundary condition, the effective action is reduced to a (2+1)D Chern-Simons term on the surface, which describes a surface QHE with half-quantized surface Hall conductance [7]. Such a topological θ term with a universal value of $\theta = \pi$ in TIs leads to a magnetoelectric effect with coefficient quantized in units of $e^2/2h$, known as the topological magnetoelectric effect (TME), i.e., an electric field can induce a magnetic polarization, whereas a magnetic field can induce an electric polarization. To obtain the quantized TME in TIs, as is first suggested in Ref. [7], one must fulfill the following stringent requirements. First, introduce a $\mathcal{T}$-breaking surface gap by ferromagnetic (FM) ordering, where the magnetization of FM points inward or outward from the surface. Second, finely tune the Fermi level into the magnetically induced surface gap and keep the bulk truly insulating. Third, the film of the TI material should be thick enough to eliminate the finite-size effect, therefore the TME is exactly quantized. Several other theoretical proposals [11–14] have been made to realize the the TME; however, observing the TME in TIs experimentally is still challenging.

In this Rapid Communication, we propose to realize the TME effect in the newly discovered quantum anomalous Hall (QAH) state [15,16]. Recently, a new zero-plateau QAH state in a magnetic TI has been theoretically predicted [17] and experimentally realized [18,19]. The magnetic TI studied in the QAH experiment develops robust FM at low temperature. In the magnetized states, the magnetic domains of the material are aligned to the same direction, and the system is in a QAH state with a single chiral edge state propagating along the sample boundary, where the Hall conductance σ_{xy} is quantized to be $\pm e^2/h$. The zero-plateau state, on the contrary, appears around the coercivity when the magnetic domains reverse, where σ_{xy} shows a well-defined zero plateau over a range of magnetic field around coercivity while the longitudinal conductance $\sigma_{xx} \to 0$ [shown in Fig. 1(a)]. In such a state, the Fermi level is in the magnetization induced surface gap, fulfilling the first two conditions above, providing a good platform to observe the TME effect, as we will discuss in detail below. However, due to a finite thickness in magnetic TIs, the TME is nonquantized. Therefore, we further propose to realize the *quantized* TME effect in the zero-plateau QAH state of the FM-TI-FM heterostructure as shown in Fig. 1(b), where an in-plane ac magnetic field induces an electric current in the same direction, or an in-plane electric field induces a magnetic field. The finite-size effect is also studied numerically, where the TME coefficient is shown to converge to a quantized value when the thickness of the TI film increases. Finally, we propose a device setup where the nontopological contribution from the side surface is negligible.

The TME described by the topological θ term implies that a quantized magnetic polarization is induced by an electric field,

 ©2015 American Physical Society

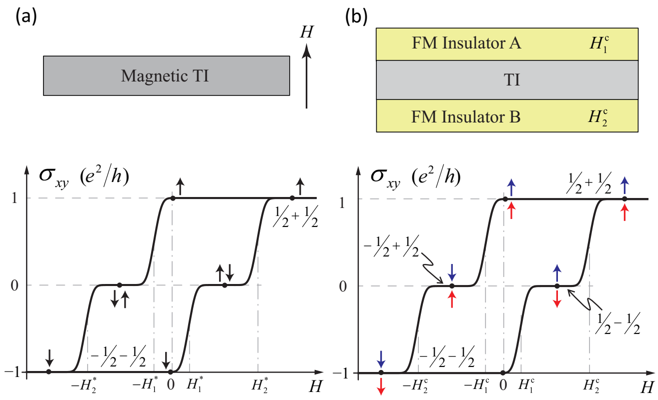

FIG. 1. (Color online) Zero-plateau QAH state and magnetic field dependence of σ_{xy}. (a) Magnetic TI in an external field H, and sketch of σ_{xy} as a function of H. The $\sigma_{xy}=0$ plateau occurs at the coercivity. The arrow indicates the magnetization direction. (b) FM-TI-FM heterostructure, and σ_{xy} vs H. The zero plateau appears in the hysteresis loop due to the different H_1^c and H_2^c of FM A and B. The blue and red arrows indicate the magnetization directions of FM A and B, respectively.

given by

$$\mathbf{M}=-\frac{\theta}{2\pi}\frac{e^2}{h}\mathbf{E}. \tag{2}$$

Such a response can be understood in terms of a surface Dirac fermion picture. With antiparallel magnetization of the two FM layers as shown Fig. 2(b), an in-plane electric field $\mathbf{E}=E_y\hat{\mathbf{y}}$ induces the Hall currents $\mathbf{J}^t=\sigma_{xy}^t\hat{\mathbf{z}}\times\mathbf{E}$ and $\mathbf{J}^b=\sigma_{xy}^b\hat{\mathbf{z}}\times\mathbf{E}$ on the top ($z=d/2$ and denoted as superscript t) and bottom (b and $z=-d/2$) surfaces, respectively. Since the surface massive Dirac fermion gives rise to half-integer Hall conductance $\sigma_{xy}^t=-\sigma_{xy}^b=(\theta/2\pi)(e^2/h)$, the currents $\mathbf{J}^t=-\mathbf{J}^b$ are opposite and form a circulating total current. Inside the sample, such a circulating current can be viewed equivalently as the surface bound current generated by a constant magnetization $\mathbf{M}=-J^t\hat{\mathbf{y}}=-(\theta/2\pi)(e^2/h)\mathbf{E}$. Therefore, the TME essentially originates from the half-quantized surface Hall conductance.

First, we examine theoretically the TME in the zero-plateau QAH state observed in experiments. The low-energy physics of this system consists of Dirac-type surface states only [17,20]. At the coercivity, both *random* magnetic domains that formed in the sample, and the exchange field Δ introduced by the FM ordering, are spatially inhomogeneous. The 3D spatial average of the exchange field vanishes ($\langle\Delta\rangle_{\text{av}}=0$). However, due to an unavoidable top-bottom asymmetry, the top and bottom surfaces may feel an opposite nonzero exchange field $\Delta^t=-\Delta^b=\Delta_0$. In this case, the zero-plateau state is described by the mean field effective model, which has a generic form as $\mathcal{H}_0=k_y\sigma_1\otimes\tau_3-k_x\sigma_2\otimes\tau_3+\Delta_0\sigma_3\otimes\tau_3+m1\otimes\tau_1$. with the basis of $|t\uparrow\rangle$, $|t\downarrow\rangle$, $|b\uparrow\rangle$, and $|b\downarrow\rangle$, where $\uparrow/\downarrow$ represent the spin up/down states, respectively. σ_i and τ_i ($i=1,2,3$) are Pauli matrices acting on the spin and layer, respectively. m describes the hybridization between the top and bottom surface states. If $m=0$, due to the opposite half-integer Hall conductance contributions from the top and bottom surfaces $\sigma_{xy}^t=-\sigma_{xy}^b=\text{sgn}(\Delta_0)(e^2/2h)$, the system has $\sigma_{xy}^{\text{tot}}=0$, which gives rise to a quantized TME, as discussed above. However, a nonzero m will mix the circulating current $\mathbf{J}^t$ and $\mathbf{J}^b$, therefore, the TME is no longer quantized. In reality, the exchange field depends very much on the microscopic details of the randomness in magnetic domains. However, we emphasize that the TME of the zero-plateau state in a magnetic TI is in general nonzero and nonquantized.

To realize the quantized TME effect, the TI film should be thick enough so that the hybridization between the top and bottom surfaces is negligible. Therefore, we propose

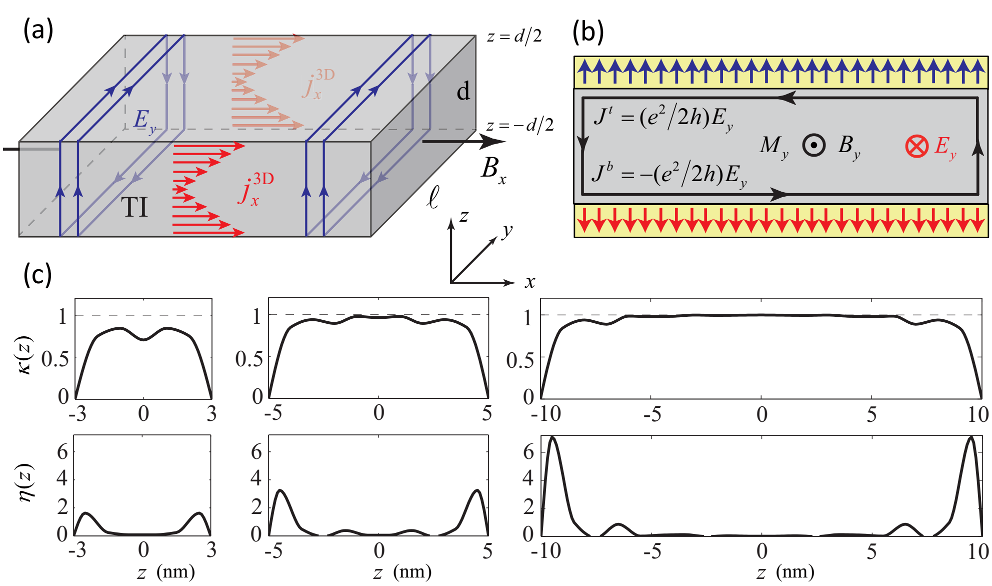

FIG. 2. (Color online) TME effect. (a) Illustration of the ac electric current induced by an ac magnetic field B_x; the current density $j_x^{3\text{D}}(z)$ is defined in Eq. (5). (b) Magnetic field B_y induced by applying an electric field E_y through a capacitor. E_y (with direction into the paper) will induce Hall currents $\mathbf{J}^t$ and $\mathbf{J}^b$ for antiparallel magnetization. (c) The functions $\kappa(z)$ and $\eta(z)$ for different thicknesses 6, 10, and 20 QL. Each QL is about 1 nm thick.

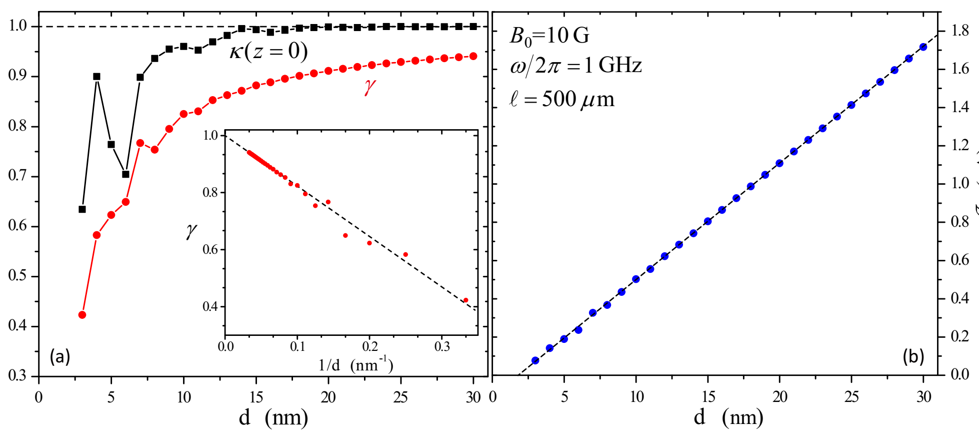

FIG. 3. (Color online) Finite-size effect of TME. (a) The γ and $\kappa(z=0)$ as a function of d. The inset shows γ plotted vs the inverse of thickness $1/d$. (b) The current amplitude $\mathcal{J}_0$ scales linearly with d. Here, $\theta/\pi = \gamma$.

that a quantized TME can be realized in the zero-plateau state of the FM-TI-FM structure as shown in Fig. 1(b). The FM insulators A and B have different coercivities H_1^c and H_2^c, respectively. Assume that both FM A and B have an out-of-plane magnetic easy axis, and the same sign of the exchange coupling parameter to the TI surface states. When A and B have antiparallel magnetization, the system is in a zero-plateau QAH state with $\sigma_{xy}^{\text{tot}} = 0$, which is contributed by $\sigma_{xy}^t + \sigma_{xy}^b$ as $(1/2 - 1/2)(e^2/h)$ or $(-1/2 + 1/2)(e^2/h)$. Such a magnetization configuration can be easily achieved in the hysteresis loop by an external field H with $H_1^c < |H| < H_2^c$, and then remove H. Experimentally, to achieve the TME in this setup, a good proximity between FM and TI is necessary. The TI material can be chosen as $Bi_ySb_{1-y}Te_3$, where the Dirac cone of the surface states is observed to be located in the bulk band gap [21]. The candidate FM materials are $Cr_2Ge_2Te_6$ (CGT), $Cr_x(Bi,Sb)_{2-x}Te_3$ (CBST) with $0.3 < x < 0.46$, and $V_x(Bi,Sb)_{2-x}Te_3$ (VBST). All of them are FM insulators with an out-of-plane easy axis, and have a good lattice match with the Bi_2Te_3 family materials. CGT is a soft FM insulator with $T_c \sim 61$ K and $H_c < 100$ Oe [22], and it also shows good proximity with Bi_2Te_3 [23]. CBST with $0.3 < x < 0.46$ is a FM insulator with $T_c = 40$–90 K and $H_c \sim 1.0 \times 10^3$ Oe [24]. VBST with $0.1 < x < 0.3$ is a FM insulator with $T_c = 30$–100 K and $H_c \sim 1.0 \times 10^4$ Oe [25].

TME. As we discussed previously, an electric field will induce a topological contribution to bulk magnetization. From the constituent equation $\mathbf{H} = \mathbf{B}/\mu - \mathbf{M}$, with $\mathbf{H} = \mathbf{0}$ and $\mathbf{B}$ continuous, we have, on the middle of the side surface (parallel to $\hat{\mathbf{z}}$), $\mathbf{B} = -\mu(e^2/2h)E_y\hat{\mathbf{y}}$. Here, μ is the material-dependent magnetic permeability. Taking $\mu \approx \mu_0$, $E_y = 10^5$ V/m, we get the magnitude of the magnetic field 2.43×10^{-6} T, which is easily detectable by present superconducting quantum interference devices (SQUIDs). The stray magnetic field effect can be well separated from the quantized TME by ac modulation of the electric field and phase-locking detection, where the ac frequency is quasistatic around 10–100 Hz. Moreover, a gradiometer sensor in SQUID could also screen the homogeneous stray field.

The TME also indicates the induction of a parallel polarization current when an ac magnetic field is applied. Consider the process of applying an ac magnetic field $\mathbf{B} = B_x\hat{\mathbf{x}}$ as shown in Fig. 2(a). A circulating electric field $\mathbf{E}$ parallel to side surface (parallel to $\mathbf{B}$) is generated due to Faraday's law of induction, where $\mathbf{E}^t = -\mathbf{E}^b = (\partial B_x/\partial t)(d/2)\hat{\mathbf{y}}$. Such an electric field will induce a Hall current density $\mathbf{j}^{2\text{D}} = \mathbf{j}_t^{2\text{D}} + \mathbf{j}_b^{2\text{D}}$, where $\mathbf{j}_t^{2\text{D}} = \sigma_{xy}^t\hat{\mathbf{z}} \times \mathbf{E}^t$ and $\mathbf{j}_b^{2\text{D}} = \sigma_{xy}^b\hat{\mathbf{z}} \times \mathbf{E}^b$. Therefore, the total current $\boldsymbol{\mathcal{J}} = \mathbf{j}^{2\text{D}}\ell = \mathcal{J}\hat{\mathbf{x}}$, where

$$\mathcal{J} = \frac{\theta}{\pi}\frac{e^2}{2h}\frac{\partial B_x}{\partial t}\ell d. \tag{3}$$

Here, d and ℓ are the thickness and width of the TI film as shown in Fig. 2(a), and $\theta \to \pi$ when d is large enough. For an estimation, take $B_x = B_0 e^{-i\omega t}$, $B_0 = 10$ G, $\omega/2\pi = 1$ GHz, $d = 20$ nm, $\theta/\pi \approx 0.91$ (the finite-size effect taken into account as in Fig. 3), and $\ell = 500$ μm, we have $\mathcal{J} = -i\mathcal{J}_0 e^{-i\omega t}$ with $\mathcal{J}_0 = 1.11$ nA, in the range accessible by transport experiments. Moreover, as shown in Fig. 3(b), the current amplitude $\mathcal{J}_0$ scales linearly with thickness d, for θ is a linear function of $1/d$ with $(1-\theta/\pi) \propto 1/d$, i.e., a thicker film gives rise to a larger TME.

Finite-size effect. Due to the finite-size confinement along the z direction, the TME effect is not quantized when the TI film is thin. However, as we shall show below, the TME coefficient converges quickly into the quantized value as the film thickness d increases. The generic Hamiltonian of a TI thin film can be written as $\mathcal{H}_{2\text{D}}(\mathbf{k}) = \int_{-d/2}^{d/2} dz \mathcal{H}_{3\text{D}}(\mathbf{k},z)$. Here, $\mathbf{k} = (k_x,k_y)$, and we impose periodic boundary conditions in both the x and y directions. The magnetoelectric response of such a thin film can be directly calculated with the Kubo formula. With the 3D in-plane current density operator defined as $\mathbf{j}^{3\text{D}}(\mathbf{k},z) = (e/\hbar)\partial_{\mathbf{k}}\mathcal{H}_{3\text{D}}(\mathbf{k},z)$, we can write down a dc current correlation function,

$$\Pi_{xy}(z,z') = \frac{\hbar^2}{2\pi e^2}\int d^2\mathbf{k}\sum_{n\neq m} f(\epsilon_{n\mathbf{k}}) \times 2\,\text{Im}\left[\frac{\langle u_{n\mathbf{k}}|j_x^{3\text{D}}(\mathbf{k},z)|u_{m\mathbf{k}}\rangle\langle u_{m\mathbf{k}}|j_y^{3\text{D}}(\mathbf{k},z')|u_{n\mathbf{k}}\rangle}{(\epsilon_{n\mathbf{k}}-\epsilon_{m\mathbf{k}})^2}\right],$$

where $|u_{n\mathbf{k}}\rangle$ is the normalized Bloch wave function in the nth electron subband satisfying $\mathcal{H}_{2\text{D}}(\mathbf{k})|u_{n\mathbf{k}}\rangle = \epsilon_{n\mathbf{k}}|u_{n\mathbf{k}}\rangle$, and $f(\epsilon)$ is the Fermi-Dirac distribution function. The Kubo formula for magnetic field B_y induced by a uniform external electric field

E_y is then given by

$$B_y(z) = -\mu \frac{e^2}{2h}\kappa(z)E_y, \tag{4}$$

where $\kappa(z) = \int_{-d/2}^{d/2} dz_1 \, \mathrm{sgn}(z - z_1) \int_{-d/2}^{d/2} dz_2 \, \Pi_{xy}(z_1,z_2)$ is a dimensionless function. Here $\mathrm{sgn}(z)$ gives the sign of z. Similarly, the current density j_x^{3D} induced by a uniform external ac magnetic field B_x of frequency $\omega/2\pi$ is given by

$$j_x^{3D}(z) = -i\omega \frac{e^2}{2h}\eta(z)B_x, \tag{5}$$

where $\eta(z) = 2\int_{-d/2}^{d/2} dz_1 \, z_1 \Pi_{xy}(z,z_1)$ is also dimensionless.

The response formulas above are generic for any TI system and do not rely on a specific model. For concreteness, we adopt the effective Hamiltonian in Ref. [26] to describe the low-energy bands of Bi_2Te_3 family materials, $\mathcal{H}_{3D}(\mathbf{k},z) = \varepsilon 1 \otimes 1 + d^1\tau_1 \otimes 1 + d^2\tau_2 \otimes \sigma_3 + d^3\tau_3 \otimes 1 - \Delta(z)\tau_3 \otimes \sigma_3 + iA_1\partial_z\tau_2 \otimes \sigma_2$. Here, τ_j and σ_j $(j = 1,2,3)$ are Pauli matrices, $\varepsilon(\mathbf{k},z) = -D_1\partial_z^2 + D_2(k_x^2 + k_y^2)$, $d^{1,2,3}(\mathbf{k},z) = [A_2k_x, A_2k_y, B_0 - B_1\partial_z^2 + B_2(k_x^2 + k_y^2)]$, and $\Delta(z)$ is the z-dependent exchange field. We then discretize it into a tight-binding model along the z axis between neighboring quintuple layers (QLs) from $\mathcal{H}_{3D}$, and assume $\Delta(z)$ takes the values $\pm\Delta_s$ in the top and bottom layers, respectively, and zero elsewhere. Figure 2(c) shows the numerical calculations of $\kappa(z)$ and $\eta(z)$ for thin films of 6, 10, and 20 QL, where we set a typical surface exchange field $\Delta_s = 50$ meV. All the other parameters are taken from Ref. [27] for $(Bi_{0.1}Sb_{0.9})_2Te_3$. The bulk value of $\kappa(z)$ at $z = 0$ as a function of d is plotted as a black line in Fig. 3. As is consistent with the topological field theory, $\kappa(z)$ in the bulk tends to 1 and becomes quantized as the thickness d increases, whereas $\eta(z)$ is bounded within a finite penetration depth to the top and bottom surfaces. The shapes of the functions $\kappa(z)$ and $\eta(z)$ near the surfaces remain almost unchanged as the thickness d varies.

To characterize the deviation from topological quantization of the TME in TI thin films, we further define the dimensionless number,

$$\gamma = \frac{1}{d}\int_{-d/2}^{d/2} dz \, \kappa(z) = \frac{1}{d}\int_{-d/2}^{d/2} dz \, \eta(z), \tag{6}$$

which is the mean value of $\kappa(z)$ or $\eta(z)$ (which are equal to each other). The average magnetic field in response to the external electric field E_y is then $B_y^{\mathrm{mean}} = -\gamma\mu(e^2/2h)E_y$, whereas the total 2D current density induced by external magnetic field B_x is given by $j_x^{2D} = \int dz j_x^{3D}(z) = -i\omega\gamma d(e^2/2h)B_x$. Compared to Eq. (3), we get $\theta/\pi = \gamma$. The value of γ as a function of d is shown as the red line in Fig. 3, where $\gamma \to 1$ with $d \to \infty$. This shows the TME effect is quantized as the system is in the thermodynamic limit. In fact, as shown in the inset of Fig. 3, the value of $1 - \gamma$ scales linearly with $1/d$ as the thickness $d \to \infty$, which indicates $\int_{-d/2}^{d/2} dz[1 - \kappa(z)] = \mathrm{const}$ when d is large enough. This is simply because the function $1 - \kappa(z)$ is nonzero only near the top and bottom surfaces, and its shape is independent of the thickness d, as shown in Fig. 2(c). Since $(1 - \gamma) \propto 1/d$, $\mathcal{J}_0 \propto \theta d = \gamma\pi d$ is a linear function of d, as is shown in Fig. 3(b).

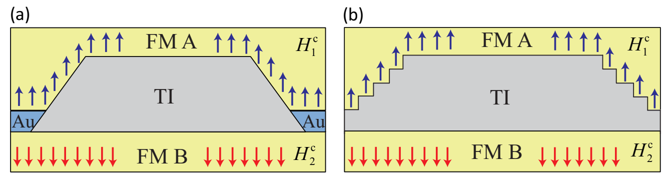

FIG. 4. (Color online) Schematic of the FM-TI-FM heterostructure to observe the quantized TME, where the side surface of the TI is gapped by a FM proximity in (a). Au is the electrode. Such a geometry of the TI can be made by lithography. In reality, such a configuration in experiments may resemble that in (b), where the side surface is uneven and steplike. In this case, the side surface is gapped by both FM ordering and quantum confinement.

Discussion. The TME effect in the setup shown in Fig. 2 is not quantized when the side surface (parallel to $\hat{\mathbf{z}}$) is not gapped. The gapless side surface states may give rise to nontopological contributions to the TME effect. To eliminate such nontopological contributions, one can use the device setup as shown in Fig. 4, where the side surface is gapped either by FM order or quantum confinement. Also in this setup, if FM A and B have opposite signs of the exchange coupling parameter to the TI surface, only parallel magnetization is needed to realize TME. Recently, the surface QHE has been realized in bulk $Bi_{2-x}Sb_xTe_{3-y}Se_y$ TIs [28,29], where the systems exhibit surface-dominated conduction even at temperatures close to room temperature, whereas the bulk conduction is negligible. Such experimental progress on the material growth and rich material choice of TI and FM insulators makes the realization of the quantized TME in TIs feasible.

Note added in proof. Recently, we became aware of an independent work on a similar problem [30]. However, their experimental proposal to observe the TME is different from our results.

We are grateful to Ke He for sharing data prior to publication, and thank Yihua Wang and Andre Broido for useful comments on the draft. This work is supported by the U.S. Department of Energy, Office of Basic Energy Sciences, Division of Materials Sciences and Engineering, under Contract No. DE-AC02-76SF00515, and in part by the National Science Foundation under Grant No. DMR-1305677. X.L.Q. is supported by the National Science Foundation through Grant No. DMR-1151786.

[1] D. J. Thouless, *Topological Quantum Numbers in Nonrelativistic Physics* (World Scientific, Singapore, 1998).

[2] N. Byers and C. N. Yang, Phys. Rev. Lett. **7**, 46 (1961).

[3] D. J. Thouless, M. Kohmoto, M. P. Nightingale, and M. den Nijs, Phys. Rev. Lett. **49**, 405 (1982).
[4] P. J. Mohr, B. N. Taylor, and D. B. Newell, Rev. Mod. Phys. **80**, 633 (2008).
[5] M. Z. Hasan and C. L. Kane, Rev. Mod. Phys. **82**, 3045 (2010).
[6] X.-L. Qi and S.-C. Zhang, Rev. Mod. Phys. **83**, 1057 (2011).
[7] X.-L. Qi, T. L. Hughes, and S.-C. Zhang, Phys. Rev. B **78**, 195424 (2008).
[8] A. M. Essin, J. E. Moore, and D. Vanderbilt, Phys. Rev. Lett. **102**, 146805 (2009).
[9] We use SI units. For CGS units, $e^2/h \to \alpha/2\pi$, where α is the fine structure constant.
[10] F. Wilczek, Phys. Rev. Lett. **58**, 1799 (1987).
[11] X.-L. Qi, R. Li, J. Zang, and S.-C. Zhang, Science **323**, 1184 (2009).
[12] J. Maciejko, X.-L. Qi, H. D. Drew, and S.-C. Zhang, Phys. Rev. Lett. **105**, 166803 (2010).
[13] W.-K. Tse and A. H. MacDonald, Phys. Rev. Lett. **105**, 057401 (2010).
[14] K. Nomura and N. Nagaosa, Phys. Rev. Lett. **106**, 166802 (2011).
[15] C.-Z. Chang, J. Zhang, X. Feng, J. Shen, Z. Zhang, M. Guo, K. Li, Y. Ou, P. Wei, L.-L. Wang, Z.-Q. Ji, Y. Feng, S. Ji, X. Chen, J. Jia, X. Dai, Z. Fang, S.-C. Zhang, K. He, Y. Wang, L. Lu, X.-C. Ma, and Q.-K. Xue, Science **340**, 167 (2013).
[16] J. Wang, B. Lian, and S.-C. Zhang, arXiv:1409.6715 [Phys. Scr. (to be published)].
[17] J. Wang, B. Lian, and S.-C. Zhang, Phys. Rev. B **89**, 085106 (2014).
[18] Y. Feng *et al.*, arXiv:1503.04569.
[19] X. Kou *et al.*, arXiv:1503.04150.
[20] J. Wang, B. Lian, and S.-C. Zhang, Phys. Rev. Lett. **115**, 036805 (2015).
[21] J. Zhang, C.-Z. Chang, Z. Zhang, J. Wen, X. Feng, K. Li, M. Liu, K. He, L. Wang, X. Chen, Q.-K. Xue, X. Ma, and Y. Wang, Nat. Commun. **2**, 574 (2011).
[22] H. Ji, R. A. Stokes, L. D. Alegria, E. C. Blomberg, M. A. Tanatar, A. Reijnders, L. M. Schoop, T. Liang, R. Prozorov, K. S. Burch, N. P. Ong, J. R. Petta, and R. J. Cava, J. Appl. Phys. **114**, 114907 (2013).
[23] L. D. Alegria, H. Ji, N. Yao, J. J. Clarke, R. J. Cava, and J. R. Petta, Appl. Phys. Lett. **105**, 053512 (2014).
[24] H. Ke (private communication). With $0.3 < x < 0.46$, the topological nontrivial properties in CBST disappear due to a high Cr concentration.
[25] C.-Z. Chang, W. Zhao, D. Y. Kim, H. Zhang, B. A. Assaf, D. Heiman, S.-C. Zhang, C. Liu, M. H. W. Chan, and J. S. Moodera, Nat. Mater. **14**, 473 (2015).
[26] J. Wang, B. Lian, H. Zhang, Y. Xu, and S.-C. Zhang, Phys. Rev. Lett. **111**, 136801 (2013).
[27] H. Zhang, C.-X. Liu, X.-L. Qi, X. Dai, Z. Fang, and S.-C. Zhang, Nat. Phys. **5**, 438 (2009).
[28] Y. Xu, I. Miotkowski, C. Liu, J. Tian, H. Nam, N. Alidoust, J. Hu, C.-K. Shih, M. Z. Hasan, and Y. P. Chen, Nat. Phys. **10**, 956 (2014).
[29] R. Yoshimi, A. Tsukazaki, Y. Kozuka, J. Falson, K. Takahashi, J. Checkelsky, N. Nagaosa, M. Kawasaki, and Y. Tokura, Nat. Commun. **6**, 6627 (2015).
[30] T. Morimoto, A. Furusaki, and N. Nagaosa, arXiv:1505.06285.